



RESEARCH ARTICLE

WILEY

Tonic GABA-activated synaptic and extrasynaptic currents in dentate gyrus granule cells and CA3 pyramidal neurons along the mouse hippocampal dorsoventral axis

Olga Netsyk | Hayma Hammoud | Sergiy V. Korol | Zhe Jin |
Atieh S. Tafreshiha | Bryndis Birnir

Department of Medical Cell Biology, Uppsala University, Uppsala, Sweden

Correspondence

Bryndis Birnir, Department of Medical Cell Biology, Uppsala University, Husargatan 3, Uppsala 75124, Sweden.
Email: bryndis.birnir@mcb.uu.se

Funding information

Excellence of Diabetes Research in Sweden (EXODIAB); Hjärnfonden; Vetenskapsrådet, Grant/Award Numbers: 2015-02417, 2018-02952

Abstract

The hippocampus is a medial temporal lobe structure in the brain and is widely studied for its role in memory and learning, in particular, spacial memory and emotional responses. It was thought to be a homogenous structure but emerging evidence shows differentiation along the dorsoventral axis and even microdomains for functional and cellular markers. We have examined in two cell-types of the hippocampal projection neurons, the dentate gyrus (DG) granule cells and CA3 pyramidal neurons, if the GABA-activated tonic current density varied between the dorsal (septal) and the ventral (temporal) poles of the male mouse hippocampus. Tonic synaptic currents, arising from spontaneous and miniature inhibitory postsynaptic currents (sIPSC, mIPSC), and extrasynaptic tonic currents were evaluated. The results revealed different levels of sIPSC but not mIPSC density between the dorsal and ventral hippocampal neurons for both the DG granule cells and the CA3 pyramidal neurons. The extrasynaptic tonic current density was larger in the DG granule cells as compared to the CA3 pyramidal neurons but did not vary between the dorsal and ventral regions. IPSC bursting was observed in both cell-types in the ventral hippocampus but was more common in the CA3 pyramidal neurons. Only in the dorsal DG granule cells was the level of the sIPSC and mIPSC density similar. The results indicate that the tonic GABAergic inhibition is particularly strong in the ventral hippocampal DG granule cells and enhanced in the dorsal as compared to the ventral hippocampal CA3 pyramidal neurons.

KEYWORDS

extrasynaptic tonic current, GABA, GABA_A receptor, inhibitory transmission, IPSC, synaptic transmission

1 | INTRODUCTION

The hippocampus is a medial temporal lobe structure critically involved in spatial memory formation and navigation, emotional responses, and regulation of body physiology (Lathe, 2001; Papatheodoropoulos, 2018;

Risold & Swanson, 1996; Strange, Witter, Lein, & Moser, 2014). It is an elongated curved structure with a longitudinal axis extending from dorsal (septal)-to-ventral (temporal) in rodents and corresponds to the posterior-to-anterior hippocampus in humans (Papatheodoropoulos, 2018; Strange et al., 2014). The dorsal hippocampus receives visual

This is an open access article under the terms of the Creative Commons Attribution License, which permits use, distribution and reproduction in any medium, provided the original work is properly cited.

© 2020 The Authors. *Hippocampus* published by Wiley Periodicals, Inc.

and spatial information from the sensory cortices whereas the ventral hippocampus has more connectivity with the prefrontal cortex, hypothalamus, and amygdala (Canteras & Swanson, 1992; Moser, Moser, & Andersen, 1993; Preston & Eichenbaum, 2013; Risold & Swanson, 1996; Strange et al., 2014). At the macroscopic level, the hippocampus appears to be a homogenous structure with a characteristic neuronal network module that is repeated in a parallel lamellar fashion along the longitudinal axis (Andersen, Bliss, & Skrede, 1971; Papatheodoropoulos, 2018). However, superimposed on the anatomical lamellar organization are molecular and functional gradients that run along the dorsoventral axis with no apparent "hard" boundaries (Fanselow & Dong, 2010; Strange et al., 2014). The hierarchies of the multiple domains that may result is currently not known. A common simplification of the endogenous diversification of the hippocampus is when the structure is divided along the dorsoventral axis into dorsal, intermediate, and ventral domains (Papatheodoropoulos, 2018; Strange et al., 2014).

Several studies have revealed variations in electrophysiological properties of hippocampal neurons along the longitudinal axis (Maggio & Segal, 2007; Malik, Dougherty, Parikh, Byrne, & Johnston, 2016; Milior et al., 2016; Papatheodoropoulos, 2015; Petrides, Georgopoulos, Kostopoulos, & Papatheodoropoulos, 2007; Schreurs, Sabanov, & Balschun, 2017). It is furthermore well-established that there is an increasing degree of neuronal excitability from the dorsal to the ventral pole of the hippocampus (Bragdon, Taylor, & Wilson, 1986; Dougherty, Islam, & Johnston, 2012; Gilbert, Racine, & Smith, 1985; Malik et al., 2016; Papatheodoropoulos, 2018; Petrides et al., 2007). The ventral hippocampus is further reported to have higher propensity for generating epileptic activity (Bragdon et al., 1986; Gilbert et al., 1985; Papatheodoropoulos, 2018). This is despite the fact that GAD67 positive cells are more numerous in the ventral as compared to the dorsal hippocampus (Hortnagl, Berger, Sperk, & Piffl, 1991; Neddens & Buonanno, 2010). Interestingly, the GABA-concentration gradient is reported to increase from dorsal to ventral for the CA1 and the CA3 hippocampal regions but, notably, not the DG regions where the concentration is similar (Hortnagl et al., 1991; Neddens & Buonanno, 2010).

A number of mechanisms have been proposed to account for the increased excitability of the ventral hippocampus, including reduced inhibitory GABAergic actions (Papatheodoropoulos, 2018). It is, nevertheless, not clear how the reduced inhibition is manifested at the cellular level as detailed investigations of dorsoventral differences of GABAergic currents are limited to-date. Tonic GABA-activated conductances in the hippocampus may result from the summation of overlapping IPSCs (Edwards, Konnerth, & Sakmann, 1990; Otis & Mody, 1992; Otis, Staley, & Mody, 1991; Soltesz, Smetters, & Mody, 1995) and from GABA_A receptors opening spontaneously or activated extrasynaptically by interstitial GABA (Bai et al., 2001; Birnir, Everitt, & Gage, 1994; Birnir, Everitt, Lim, & Gage, 2000; Brickley, Cull-Candy, & Farrant, 1996; Rossi & Hamann, 1998; Semyanov, Walker, & Kullmann, 2003; Wlodarczyk et al., 2013). Currents driven by spontaneous activity of interneurons are termed sIPSCs and the action-potential independent currents, mIPSCs (Edwards et al., 1990;

Otis et al., 1991; Otis & Mody, 1992; Soltesz et al., 1995). Here we have compared the tonic GABA-activated synaptic and the extrasynaptic currents in DG granule cells and CA3 pyramidal neurons from the dorsal and ventral mouse hippocampus, as more is known about the inhibitory drive onto CA1 pyramidal neurons at the two hippocampal poles (Milior et al., 2016; Papatheodoropoulos, Asproдини, Nikita, Koutsona, & Kostopoulos, 2002; Petrides et al., 2007; Schreurs et al., 2017; Sotiriou, Papatheodoropoulos, & Angelatou, 2005). The results are consistent with cell-type, DG granule cell, or CA3 pyramidal neuron, specific variation in the tonic inhibitory level along the dorsoventral axis of the mouse hippocampus.

2 | MATERIALS AND METHODS

2.1 | Animals

All experiments were performed in accordance with the local ethical guidelines and protocols approved by Uppsala animal ethical committee, Swedish law and regulations based on the Directive 2010/63/EU. C57BL/6J male mice (Taconic M&B, Denmark), 8–10 weeks old, were used in all experiments. For the DG granule cells, hippocampal slices from 74 mice were used to record from dorsal hippocampus (DH, 37 mice) and ventral hippocampus (VH, 43 mice). From six mice, data was obtained for both DH and VH. For the CA3 pyramidal neurons, hippocampal slices from 77 mice were used to record from DH (53 mice) and VH (45 mice). From 21 mice, data was obtained for both DH and VH.

2.2 | Brain slice preparation

Mice were euthanized by cervical dislocation and then decapitated. The brain slices were prepared according to the procedure described by Ting et al. (2014) and Jin et al. (2011). Briefly, the brain was quickly removed and placed into ice-cold *N*-methyl *D*-glucamine (NMDG)-based cutting solution containing (in mM): 93 NMDG, 2.5 KCl, 1.2 NaH₂PO₄, 30 NaHCO₃, 20 4-(2-hydroxyethyl)piperazine-1-ethanesulfonic acid (HEPES), 25 *D*-glucose, 10 MgSO₄, 0.5 CaCl₂, 5 sodium ascorbate, 2 thio-urea, 3 sodium pyruvate, pH 7.3–7.4 adjusted with HCl when saturated with 95% O₂ and 5% CO₂, osmolarity 300–305 mOsm adjusted with sucrose. The cerebellum and one-third of each hemisphere from the rostral pole of the brain were removed and a cut was made along the midline to separate the hemispheres. The hippocampal slices (350 μm thick) were cut with a microtome (Leica VT1200 S, Leica Microsystems AB, Germany).

Dorsal and ventral DG were defined in coronal slices according to Paxinos and Watson (1986). Hippocampal slices including the dorsal CA3 region were obtained by cutting the hemisphere in the coronal plane (the coronal sections) and the first three hippocampal slices were collected from the dorsal pole. For the ventral hippocampal slice preparation, the hemisphere was mounted on the flat dorsal surface. The first four horizontal hippocampal slices were collected from the

ventral region of the brain. The slices were then placed into chamber filled with the NMDG-based solution and incubated for 12–15 min at 32°C. After that, the slices were transferred to the incubation chamber filled with the HEPES-based holding solution (in mM): 92 NaCl, 2.5 KCl, 1.2 NaH₂PO₄, 30 NaHCO₃, 20 HEPES, 25 D-glucose, 2 MgSO₄, 2 CaCl₂, 5 sodium ascorbate, 2 thiourea, 3 sodium pyruvate, pH 7.3–7.4 adjusted with NaOH when saturated with 95% O₂ and 5% CO₂; osmolarity 300–305 mOsm adjusted with sucrose. The slices were kept in the holding solution at room temperature (20–22°C) for at least 1 hr before use.

2.3 | Slice electrophysiology

Whole-cell patch-clamp recordings (Jin, Jin, & Birnir, 2011) were performed on DG granule cells and CA3 pyramidal neurons from dorsal and ventral regions of the hippocampus in the mouse brain slices. DG granule cells in suprapyramidal and infrapyramidal blades and pyramidal neurons located in the middle of the proximodistal (DG-CA2) axis of CA3 region were targeted for recordings. All experiments were conducted at room temperature. Before experiments, the slice was transferred to the recording chamber and perfused (1.5–2 ml/min) with artificial cerebrospinal fluid (ACSF) containing (mM): 119 NaCl, 2.5 KCl, 1.3 MgSO₄, 1 NaH₂PO₄, 26.2 NaHCO₃, 2.5 CaCl₂, 11 D-glucose, and 3 kynurenic acid, pH 7.3–7.4 equilibrated with 95% O₂ and 5% CO₂, osmolarity 300–303 mOsm adjusted with sucrose. Borosilicate glass patch pipettes were filled with an intracellular solution containing (mM): 140 CsCl, 8 NaCl, 2 EGTA, 0.2 MgCl₂, 10 HEPES, 2 MgATP, 0.3 Na₃GTP, 5 QX314Br, pH 7.2 adjusted with CsOH, osmolarity 285–290 mOsm. The pipette resistance was 3.4–4.0 MΩ when filled with the intracellular solution. The blind patch-clamp technique was used (Jin, Jin, & Birnir, 2011) and data collection was started 10–15 min after obtaining the whole-cell configuration and the recording had stabilized. Voltage-clamp recordings were made at the holding potential of –60 mV and filtered at 2 kHz using Axoclamp 200B amplifier/Multipatch 700B amplifier (Axon Instruments, Molecular Devices, CA) and Axon Digidata board 1440A/1550A (Molecular Devices) controlled by pCLAMP 10.5 software (Axon Instruments, Molecular Devices). To isolate GABA_AR-mediated currents 3 mM kynurenic acid was added to the ACSF to block the glutamatergic synaptic transmission.

sIPSCs were recorded for at least 5 min after baseline stabilization. For mIPSCs recordings, tetrodotoxin (TTX, 1 μM, bath application for 10–12 min) was added to the ACSF to block voltage-activated sodium channels and, therefore, action potential-dependent GABA release (Edwards et al., 1990). To reveal the extrasynaptic GABA_A receptors mediated tonic currents, 100 μM picrotoxin or bicuculline methiodide was applied.

2.4 | Drugs

Chemicals and drugs were purchased from Sigma-Aldrich (Steinheim, Germany) apart from TTX (Alomone labs Ltd., Jerusalem, Israel).

Picrotoxin was dissolved in dimethyl sulfoxide (DMSO). The concentration of DMSO in the ACSF was 0.1% (v/v).

2.5 | Data analysis

The sIPSCs and mIPSCs were analyzed using the MiniAnalysis software 6.0 (Synaptosoft, Decatur). IPSC events were first detected if larger than a threshold value, which was set as 5xRMS (root-mean-square of the baseline noise), and then visually inspected to remove false events. As the frequency of IPSCs differs between DG granule cells and CA3 pyramidal neurons, we used time (3–5 min) and number of events (200–300 events), respectively, for the analysis. Only IPSC events with a single peak were used for analysis of amplitude and kinetics of the currents (10–90% rising time <5 ms, current decay (ms), charge transfer Q (fC), Figure S1a). The total synaptic current (sIPSC_T or mIPSC_T) was defined as frequency (s⁻¹) × Q (fC) for the individual neuron. To account for variable cell size, the IPSC_T was normalized to the cell membrane capacitance (Cm (pF)) and expressed as total synaptic current density, sIPSC_T density or mIPSC_T density (pA/pF), Figure S1b. Immature granule cells can be electrophysiologically identified based on the high membrane resistance and relatively small cell membrane capacitance (Overstreet-Wadiche & Westbrook, 2006; Pedroni, Minh do, Mallamaci, & Cherubini, 2014). Only four immature granule cells were identified and these cells were recorded in the DH (sIPSCs frequency = 0.088 ± 0.013 Hz, Rm = 1.325 ± 0.225 GΩ, Cm = 17.11 ± 4.431 pF) and were not included in the current study. For analysis of recurrent bursting activity of synaptic events obtained from DG granule cells and CA3 pyramidal neurons, at least 3–5 consecutive bursts were selected from individual cells and analyzed using the pCLAMP 10.5 software (Axon Instruments, Molecular Devices). The individual bursts were identified as high frequency and high amplitude IPSCs. The bursts were separated by basal sIPSC activity. In order to characterize recurrent bursting activity, we determined burst parameters, that is, burst frequency, interburst interval, and burst charge transfer (burst Q). The total bursts current was determined according to burst_T (pA) = burst frequency (s⁻¹) × burst Q (pC) and the density, burst_T density (pA/pF) = burst_T (pA)/Cm (pF). In total, we analyzed 14 individual bursts from 5 DG granule cells and 81 bursts from 19 CA3 neurons. The values from each burst were averaged per cell to obtain the mean value for the individual neuron. The extrasynaptic tonic current amplitude was measured as the shift of baseline at the holding current after application of a GABA_A receptors inhibitor, picrotoxin, or bicuculline (Bai et al., 2001; pCLAMP 10.5 software, Axon Instruments, Molecular Devices). To account for size variation among the cells, the extrasynaptic tonic current density was expressed as the extrasynaptic tonic current amplitude normalized to the cell membrane capacitance (Stell, Brickley, Tang, Farrant, & Mody, 2003), Figure S1b.

2.6 | Statistics

The data were analyzed using the GraphPad Prism 8 (GraphPad Software La Jolla, CA). Values are presented as mean ± SEM, *n* refers to

the number of analyzed cells. All data were included in the analysis unless statistically defined as outliers by the Tukey method. Each group of the data sets was tested for normality with the D'Agostino test and histogram distribution. To compare the normally distributed data, the Student's two-tailed *t*-test was used to determine statistical

differences between two experimental groups. Data sets that are not normally distributed were compared using a nonparametric Mann-Whitney *U*-test. Correlations between variables were assessed using a nonparametric Spearman rank correlation. A *p*-value less than .05 was statistically significant.

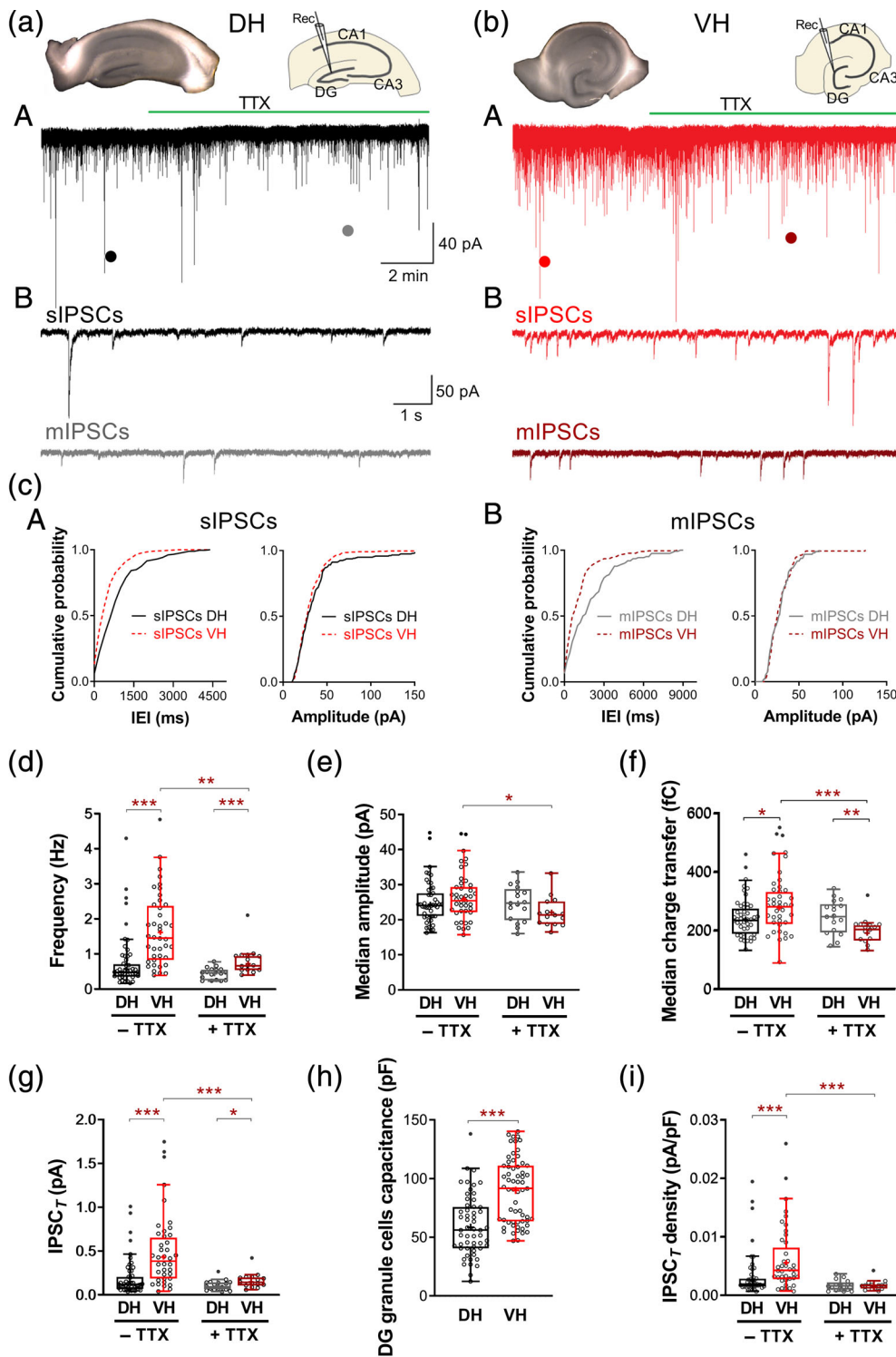


FIGURE 1 Legend on next page.

3 | RESULTS

3.1 | IPSCs differ between dorsal and ventral hippocampal neurons

The dorsal and ventral parts of the local hippocampal neuronal networks participate in different extended circuitries (Papatheodoropoulos, 2018; Strange et al., 2014) and hence, the inhibitory input of the intrinsic primary hippocampal circuitry may vary and differentially regulate the local network. To gain insight into the inhibitory regulation of the local hippocampal circuitry, we examined the functional characteristic of the IPSCs in DG granule cells (Figure 1) and CA3 pyramidal neurons (Figure 2) in the dorsal and ventral hippocampus.

3.1.1 | DG granule cells

Characteristic current traces are shown in Figure 1 on a slow (min) and a fast (s) time-scale for the dorsal (Figure 1a) and ventral (Figure 1b) DG granule cells. The frequency of both the sIPSCs and mIPSCs was higher in the ventral as compared to the dorsal hippocampus (Figure 1a–d) whereas the amplitudes of the currents were similar (Figure 1c,e). The relative frequency of the sIPSCs and mIPSCs in the dorsal to the ventral neurons was about 0.35 and 0.60, respectively. The application of TTX (1 μ M) decreased only the ventral DG granule cells IPSCs frequency by 55%, and the median amplitude by 15%. The suprapyramidal and infrapyramidal blades are defined anatomically in the DG region and they have different connectivity patterns. We further subdivided the DG data and compared the sIPSCs from the two blades but the results were comparable to those for the combined data-set (Figure S2). Further analysis of the IPSC kinetic parameters showed that the median rise times of the sIPSCs and mIPSCs from the two regions were similar whereas the median decay time and the median charge transfer varied (Figures S3 and 1f). In the ventral hippocampus, the median charge transfer was decreased by 30% by TTX (Figure 1f)

The sIPSC_T (Figure 1g) was larger in the ventral DG granule cells. This raised the question whether the current density varied, or not,

between the cells in the dorsal and ventral hippocampus. In order to estimate the neuronal size which may vary along the dorsoventral axis, we recorded the cell membrane capacitance. The DG granule cells membrane capacitance was larger, on the average, in the ventral as compared to the dorsal hippocampus (Figure 1h). The current density for cells from the two hippocampal regions is shown in Figure 1i. It revealed that the sIPSC_T density in the ventral DG granule cells was \sim 2.3 fold larger than that of the dorsal DG granule cells. Interestingly, the sIPSC_T density and the mIPSC_T density were similar for the dorsal neurons.

3.1.2 | CA3 pyramidal neurons

Characteristic current traces are shown in Figure 2 on a slow (min) and a fast (s) time-scale for the dorsal (Figure 2a) and ventral (Figure 2b) CA3 pyramidal neurons. The frequency of the sIPSCs was similar in the dorsal and ventral CA3 pyramidal neurons (Figure 2a–d). In TTX (1 μ M), the IPSCs frequency decreased (\sim 25–35%) but the mIPSCs frequency was nevertheless greater, about 1.4 fold, in the ventral as compared to the dorsal CA3 pyramidal neurons (Figure 2a–d). In contrast, both the median sIPSCs and mIPSCs amplitudes increased about 1.2 and 1.4 fold, respectively, in the dorsal as compared to ventral CA3 pyramidal neurons (Figure 2a–c,e). In TTX, the IPSCs amplitudes decreased (\sim 15–30%) in both the dorsal and ventral CA3 pyramidal neurons (Figure 2a–c,e). Further analysis of the IPSCs kinetic parameters showed that the median rise time increased for the mIPSCs in the ventral CA3 pyramidal neurons but not for the sIPSCs and the median decay times were similar for the IPSCs in the dorsal and ventral pyramidal CA3 neurons (Figure S4). The IPSCs median charge transfer was decreased in the ventral as compared to the dorsal CA3 pyramidal neurons and decreased by TTX for both hippocampal regions (Figure 2f)

The IPSC_T (Figure 2g) was similar in the CA3 pyramidal neurons from the two hippocampal regions. However, the ventral CA3 pyramidal neurons membrane capacitance was, on the average, larger than the dorsal CA3 neurons (Figure 2h) resulting in lower sIPSC_T density in the ventral CA3 pyramidal neurons (\sim 40%) as compared to the dorsal neurons (Figure 2i).

FIGURE 1 GABA_A receptor-mediated synaptic currents in DG granule cells in the mouse dorsal and ventral hippocampus. Microphotographs of a dorsal (a, DH) and a ventral (b, VH) hippocampal slices and corresponding schematic drawings to illustrate recording pipette (Rec) positioning. Representative current traces of sIPSCs and mIPSCs (1 μ M TTX) were recorded from the DG granule cells of the DH (aA) and the VH (bA). Regions marked with filled circles are shown on an expanded scale in (B). $V_{\text{hold}} = -60$ mV. (c). Cumulative probability plots for the interevent interval (IEI) and median amplitude of (A) sIPSCs (left, IEI: 259/442 events for the DH/VH; Amplitude: 175/303 events for the DH/VH) and (B) mIPSCs (right, IEI: 124/232 events for the DH/VH; Amplitude: 80/156 events for the DH/VH) recorded from DG granule cell of the DH and the VH, from the representative traces in (a) and (b). Summary graphs for the mean frequency (d), the median amplitude (e), the median charge transfer (f), and the total synaptic current (g, IPSC_T) of sIPSCs (–TTX) and mIPSCs (+TTX) recorded from DG granule cells of the DH and the VH. (h) The membrane capacitance of DG granule cells in the VH was significantly higher compared with the DH (DH vs VH: 58.5 ± 3.2 n = 54 vs 89.9 ± 3.5 n = 61, $p < .001$). (i) The sIPSCs (–TTX) and mIPSCs (+TTX) total current density recorded from the DG granule cells of the dorsal and ventral regions. Data is presented as a scatter dot plot for cell values and a box and whiskers plot with a median value plotted as a line and a mean value shown as “+.” Outliers are marked as dot plot (filled black circles) and defined by the Tukey method. Statistical analysis was performed by excluding outliers and only statistically significant differences are marked on the graph. In total, records from 46/41 granule cells in the DH/VH, respectively, were analyzed for sIPSCs (–TTX) and 17/15 granule cells in the DH/VH, respectively, were analyzed for mIPSCs (+TTX). Unpaired Students *t*-test/nonparametric Mann–Whitney *U*-test, * $p < .05$, ** $p < .01$, *** $p < .001$ [Color figure can be viewed at wileyonlinelibrary.com]

3.2 | Extrasynaptic tonic-current density is cell-type dependent

Baseline excitability of neuronal networks is regulated by a number of mechanisms including the extrasynaptic tonic GABA-activated currents

(Bai et al., 2001; Birnir et al., 1994, 2000; Brickley et al., 1996; Pavlov, Savtchenko, Kullmann, Semyanov, & Walker, 2009; Rossi & Hamann, 1998; Wlodarczyk et al., 2013). We examined if the extrasynaptic tonic-current density differed for cells along the longitudinal hippocampal axis and between the DG granule cells and the CA3 pyramidal neurons.

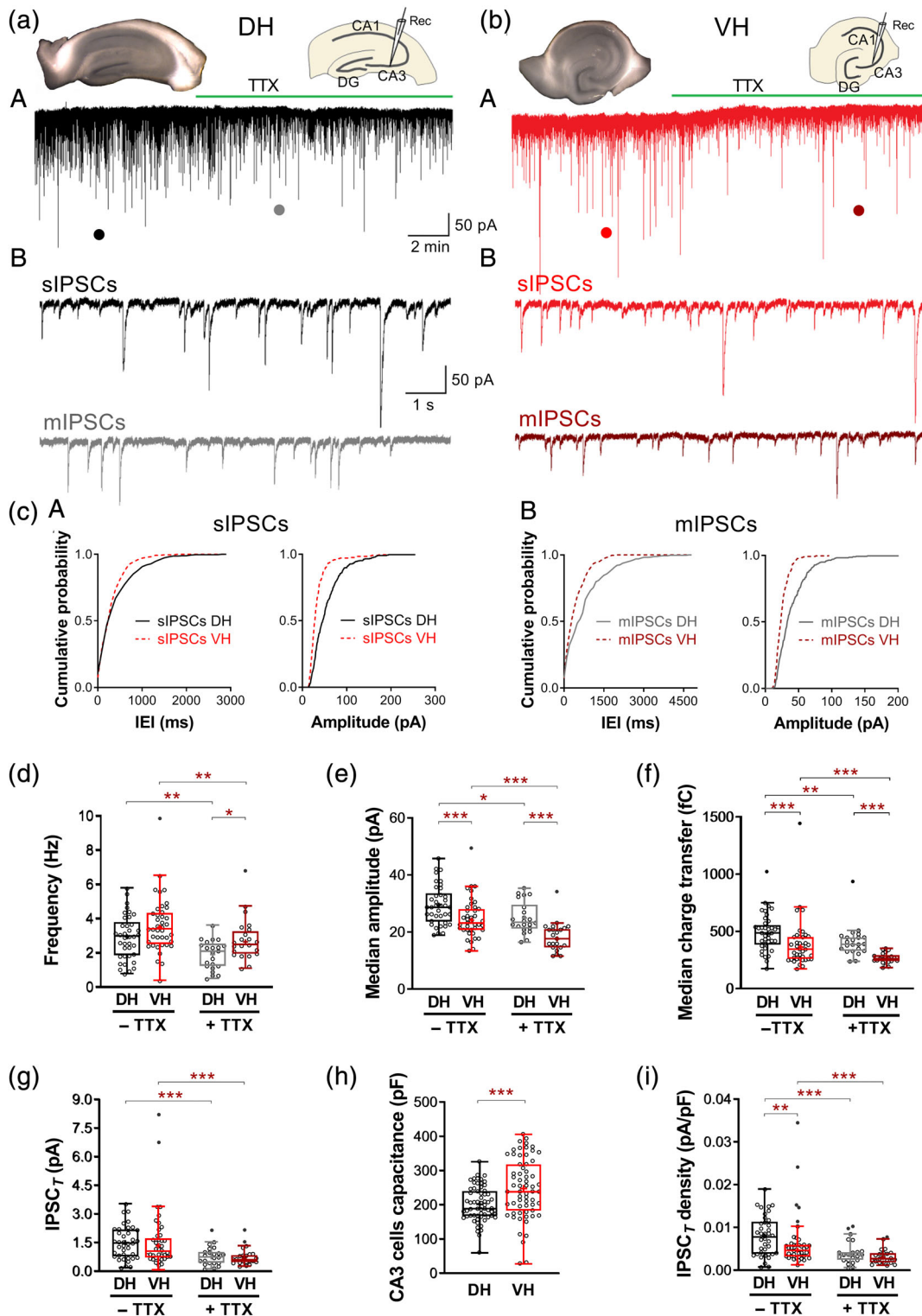


FIGURE 2 Legend on next page.

3.2.1 | DG granule cells

Extrasynaptic tonic current identified as a shift of the baseline currents with picrotoxin or bicuculline is shown in Figure 3a for a dorsal and a ventral hippocampal DG granule cell. As the neurons vary in membrane capacitance (Figure S5a), the current density was calculated by dividing the tonic current amplitude by the membrane capacitance of the cell. No difference was observed between the dorsal and ventral DG granule cells extrasynaptic tonic-current density but addition of TTX (1 μ M) significantly decreased the tonic current by \sim 31% in the ventral, but not the dorsal, DG granule cells (Figure 3c).

3.2.2 | CA3 pyramidal neurons

Typical extrasynaptic tonic currents are shown in Figure 3b for hippocampal dorsal and ventral CA3 pyramidal neurons. The extrasynaptic tonic-current density for the dorsal and ventral CA3 pyramidal neurons was similar and TTX (1 μ M) had no effect on the level of the extrasynaptic tonic-current density in these neurons (Figures 3c and S5b). It was notable that the level of the extrasynaptic tonic-current density was significantly lower in the CA3 neurons compared to the DG granule cells, by \sim 40% in the dorsal and \sim 60% in the ventral hippocampal neurons (Figure 3c).

Furthermore, in the ventral DG granule cells, the extrasynaptic tonic current density did correlate with the sIPSC density ($r_s = 0.857$, $n = 7$, $p < .05$) but not in the dorsal DG granule cells or the CA3 pyramidal neurons in dorsoventral hippocampal subregions.

3.3 | Bursts of IPSCs in the dorsal and ventral hippocampal neurons

In 10% of the DG granule cells from the ventral hippocampus (Figure 4a), large-amplitude IPSCs bursting activity was recorded in contrast to the dorsal hippocampal DG granule cells (Figures 4aB and S6a) where none were observed. A representative current trace is shown in Figure 4aA. The bursts₇ density in the cells was about 0.033

pA/pF (Figure 4aC) and the interburst interval was 75 ± 13 s ($n = 5$, Figure S6a). In the CA3 pyramidal neurons, bursts were recorded both in the dorsal and ventral CA3 pyramidal neurons and representative current traces are shown in Figure 4bA. In the dorsal hippocampus, 8% of the CA3 pyramidal neurons had recurrent IPSCs bursting activity whereas 32% of the neurons in the ventral hippocampus (Figures 4bB and S6b). The bursts₇ density was about 0.027 pA/pF and 0.016 pA/pF in the dorsal and ventral hippocampus, respectively (Figure 4bC). The interburst interval was shorter in the dorsal (20 ± 2 s, $n = 4$) as compared with the ventral hippocampal neurons (60 ± 7 s, $n = 14$).

4 | DISCUSSION

This study contributes to growing evidence revealing variable electrophysiological properties of the characteristic network module that is repeated, in a parallel lamellar fashion, along the dorsoventral axis of the hippocampus (Papatheodoropoulos, 2018; Strange et al., 2014). The results indicate that the tonic GABAergic inhibition is particularly strong in the ventral hippocampal DG granule cells and enhanced in the dorsal as compared to the ventral hippocampal CA3 pyramidal neurons (Figure 5).

The sIPSCs and mIPSCs median charge transfer differed between the dorsal and ventral hippocampus for both cell-types but so did the membrane capacitance, consistent with the DG granule cells and the CA3 pyramidal neurons being larger in the ventral hippocampus. The resulting GABA-activated current density in the neurons differed only for the sIPSC. In the DG granule cells, the ventral sIPSC₇ density was larger, in contrast, in CA3 pyramidal neurons, the dorsal sIPSC₇ density was greater. The bursts of large-amplitude sIPSCs activity followed a similar pattern. The mechanisms underlying the enhanced GABAergic spontaneous inhibitory actions in the dorsal CA3 and the ventral DG neurons are not clear but it is possible that the intrinsic excitability of the interneurons varies (Freund & Buzsaki, 1996; Papatheodoropoulos, 2018). It is well-known that neurogenesis in adult mice also has a dorso-ventral gradient with more neurogenesis in dorsal DG region (Overstreet-Wadiche & Westbrook, 2006; Pedroni et al., 2014) but immature neurons have distinct electrophysiological properties and the

FIGURE 2 GABA_A receptor-mediated synaptic currents in CA3 pyramidal neurons in the mouse dorsal and ventral hippocampus. Microphotographs of a dorsal (a, DH) and a ventral (b, VH) hippocampal slices and corresponding drawings depict schematic recording pipette (Rec) positioning. Voltage-clamp recordings of sIPSCs and mIPSCs (1 μ M TTX) in the CA3 pyramidal neurons of the DH (aA) and VH (bA) hippocampus at a holding potential of -60 mV. Regions marked with filled circles are shown on an expanded scale in (B). (c) Cumulative probability distribution for the interevent interval (IEI) and the median amplitude of (A) sIPSCs (left, IEI: 378/275 events analyzed for the DH/VH; Amplitude: 315/242 events analyzed for the DH/VH) and (B) mIPSCs (right, IEI: 333/300 events analyzed for the DH/VH; Amplitude: 277/252 events analyzed for the DH/VH) recorded from CA3 principal neuron of the DH and VH, from the representative traces (a) and (b). Summary plots for the mean frequency (d), the median amplitude (e), the median charge transfer (f), and the total synaptic current (g, IPSC₇) of sIPSCs ($-$ TTX) and mIPSCs ($+$ TTX) recorded from CA3 pyramidal neurons of the DH and the VH. (h) The membrane capacitance of CA3 neurons was significantly higher in the VH compared with the DH (DH vs. VH: 201.6 ± 6.4 n = 63 vs. 248.1 ± 11.1 n = 63, $p < .001$). (i) The total current density of the sIPSCs ($-$ TTX) and mIPSCs ($+$ TTX) recorded from the CA3 pyramidal neurons of the DH and the VH. Data is presented as a scatter dot plot for neuron values and a box and whiskers plot with a median value plotted as a line and a mean value shown as "+." Outliers, defined by the Tukey method, are marked as dot plot (filled black circles). Statistical analysis was performed by excluding outliers and only statistically significant differences are marked on the graph. In total, the records from 38/40 CA3 neurons in the DH/VH, respectively, were analyzed for sIPSCs ($-$ TTX) and 22/22 CA3 neurons in the DH/VH, respectively, were analyzed for mIPSCs ($+$ TTX). Unpaired students *t*-test/nonparametric Mann-Whitney *U*-test, * $p < .05$, ** $p < .01$, *** $p < .001$ [Color figure can be viewed at wileyonlinelibrary.com]

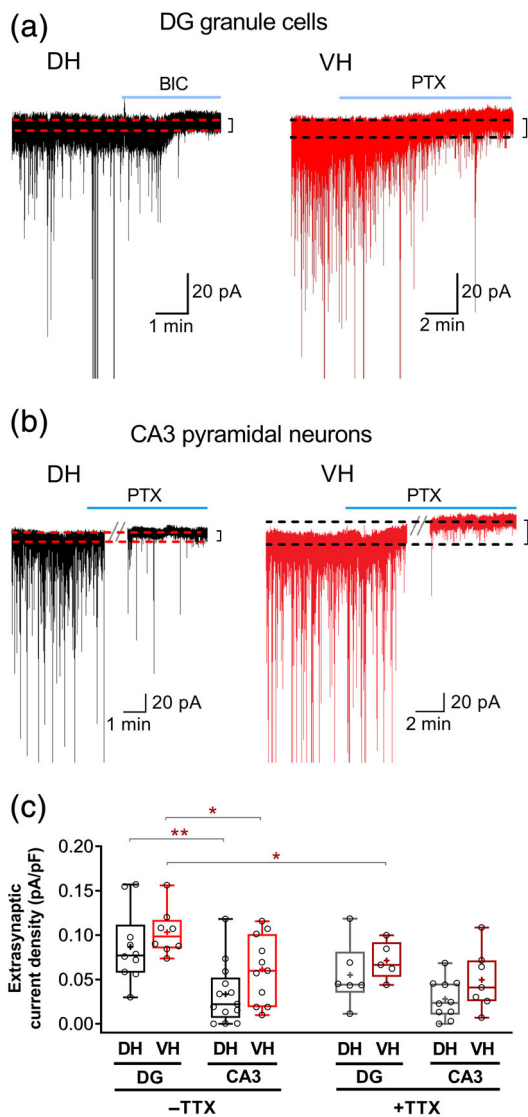


FIGURE 3 Extrasynaptic GABA_A receptor-mediated tonic currents in hippocampal DG granule cells and CA3 pyramidal neurons in the mouse dorsal and ventral hippocampus. (a). GABA-evoked tonic currents recorded in DG granule cells of the DH (dorsal hippocampus, black trace) and VH (ventral hippocampus, red trace). (b). GABA-evoked tonic currents from CA3 pyramidal neurons of the DH (black trace) and VH (red trace) under basal physiological conditions. (c). GABA-evoked extrasynaptic tonic-current density in DG granule cells and CA3 neurons from the DH and VH in the absence (–TTX) or presence of TTX (+TTX 1 μM, acute application). Upward shift of the baseline with the application of an inhibitor (picrotoxin, PTX or bicuculline, BIC, 100 μM) reveals the extrasynaptic tonic-current amplitude (the difference between the dashed lines). Data is presented as a scatter dot plot for individual cells and a box and whiskers plot with median values plotted by Tukey's method. Mean values shown as "+." Only statistically significant differences are marked on the graph. Records from 5 to 13 neurons in the DH and VH were analyzed in the absence/presence of TTX. Nonparametric Mann–Whitney *U*-test, **p* < .05; ***p* < .01. $V_{\text{hold}} = -60$ mV [Color figure can be viewed at wileyonlinelibrary.com]

four, dorsal DG immature granule cells we identified were not included in the current analysis. Nevertheless, because subpopulations of DG granule cells in the DH can be at different stages of maturation, this may contribute to the lower synaptic current density in dorsal compared with ventral DG. The similar mIPSC_T density in a given cell-type along the dorsoventral axis despite the increased mIPSC frequency in the ventral hippocampal neurons may potentially be related to more inhibitory synapses on larger neurons in the ventral hippocampus (Freund & Buzsaki, 1996; Neddens & Buonanno, 2010).

The dendritic and perisomatic inhibitory systems are anatomically and functionally segregated and differentially regulate the activity of the principal neurons in the hippocampus (Edwards et al., 1990; Freund & Buzsaki, 1996; Miles, Toth, Gulyas, Hajos, & Freund, 1996; Otis et al., 1991; Soltesz et al., 1995). Whole-cell recordings from soma (Miles et al., 1996; Otis et al., 1991; Soltesz et al., 1995) and local recordings from apical and basal dendrites (Andrasfalvy & Mody, 2006; Cossart et al., 2000) in hippocampal neurons have confirmed two functionally segregated inhibitory systems in the neurons. Somatic recordings of DG granule cells and pyramidal neurons have shown that the majority of the IPSCs recorded originate from synapses close to or at the soma (Cossart et al., 2000; Miles et al., 1996; Soltesz et al., 1995; Williams, Buhl, & Mody, 1998), and are particularly effective in controlling the output of the cells. Indeed, it has been shown that removal of the bulk of the dendritic tree (>50%) does not change the characteristics of mIPSCs recorded at the soma (Soltesz et al., 1995). In contrast, IPSCs generated in the dendrites originate from firing of dendritic projecting interneurons and primarily serve to control local excitatory conductance's and their impact on somatic output as distance-dependent scaling of the IPSCs does not take place (Andrasfalvy & Mody, 2006; Cossart et al., 2000; Miles et al., 1996; Soltesz et al., 1995). Accordingly, the majority of the results in this study are expected to originate from synapses at or close to the soma and impact sodium-dependent action potential generation in the DG granule and CA3 pyramidal neurons. This study identified a significantly higher sIPSC_T density as compared to the mIPSC_T in both the dorsal and the ventral hippocampal CA3 pyramidal neurons whereas the sIPSC_T density was only larger than the mIPSC_T in the ventral hippocampal DG granule cells. For both cell-types, where the current density was amplified, then the sIPSCs frequency and median amplitude were also increased as compared to the mIPSCs. The finding that in the dorsal hippocampus, in the DG granule cells the spontaneous and the action-potential independent IPSC_T density were similar, is consistent with a low level of spontaneous firing by the interneurons synapsing on the soma of the dorsal DG granule cell. The difference, or lack there-of, between the sIPSCs and mIPSCs observed may be related to the suggestion that GABA can regulate neuronal activity by evoking either hyperpolarization or depolarization in a dose-dependent manner that may be activity dependent (Freund & Buzsaki, 1996; Staley & Mody, 1992; Staley, Soldo, & Proctor, 1995). Intense IPSCs activity may result in shift of the chloride reversal potential to more depolarized values due to increased chloride concentration in the postsynaptic cell. Where no difference between sIPSCs and mIPSCs was recorded that is, in the dorsal hippocampal

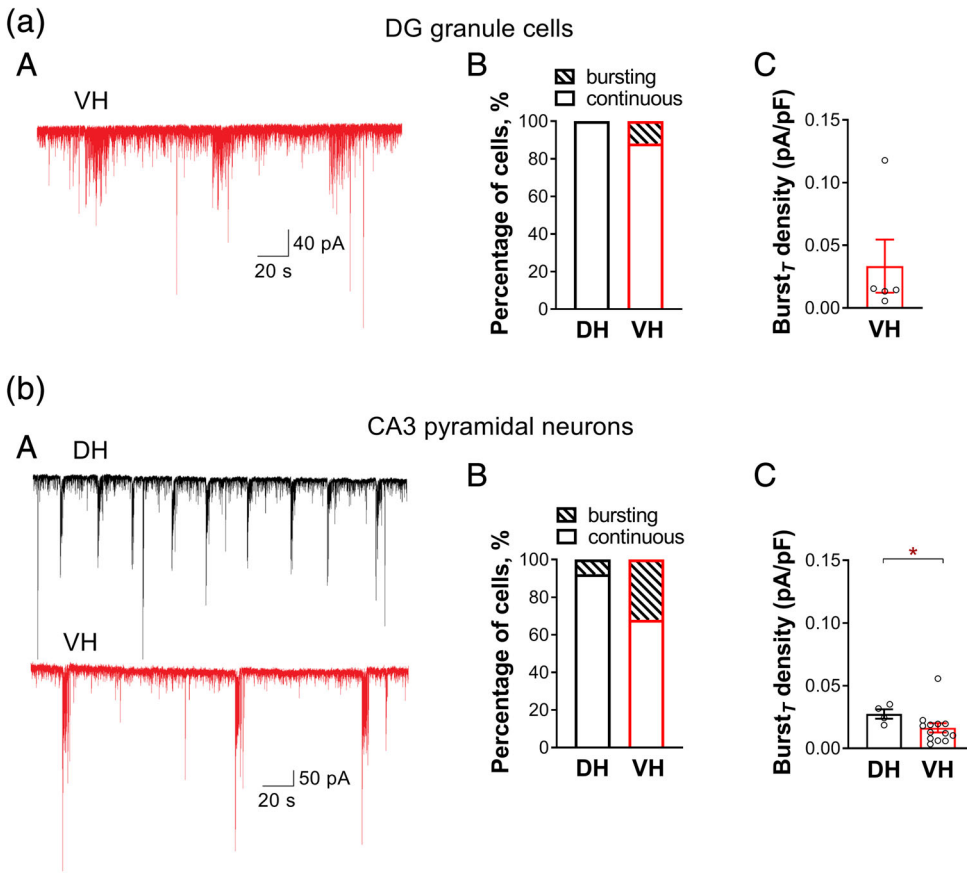


FIGURE 4 Bursting patterns of GABA-evoked large-amplitude IPSCs in DG granule cells and CA3 pyramidal neurons in the mouse dorsal and ventral hippocampus. (a). (A) Representative current record with synaptic bursting activity in mouse DG granule cell in the VH (ventral hippocampus). (B) Percent of cells exhibiting continuous or bursting synaptic currents in DG granule cells in the DH (dorsal hippocampus, $n = 46$) and VH ($n = 42$). (C) Total burst (burst_7) density in DG granule cells of the VH. (b). (A) Representative current record with synaptic bursting activity recorded in mouse CA3 pyramidal neurons in DH and VH. (B) Percent of cells exhibiting continuous or bursting synaptic currents in CA3 principal neurons in DH ($n = 51$) and VH ($n = 56$). (C) Total burst (burst_7) density in DH and VH. Data is presented as a scatter dot plot with mean \pm SEM values. Nonparametric Mann–Whitney U -test, $*p < .05$. $V_{\text{hold}} = -60$ mV [Color figure can be viewed at wileyonlinelibrary.com]

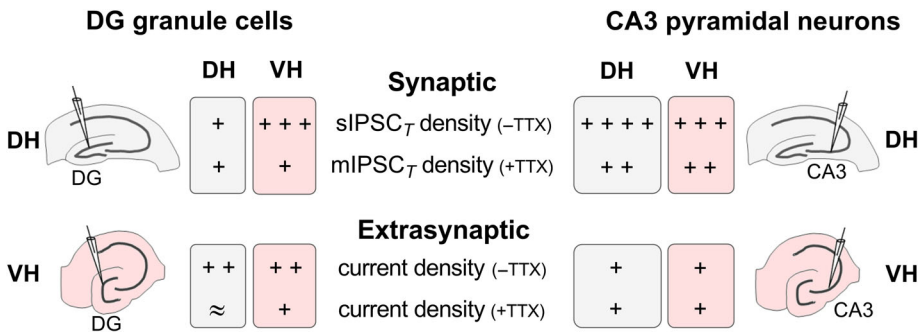


FIGURE 5 A cartoon showing relative strength of GABA-activated tonic current densities in hippocampal neurons. Electrodes identify relevant recording hippocampal areas. DH, dorsal hippocampus; VH, ventral hippocampus. Relative strength: $+ < ++ < +++ < ++++$, similar strength: \approx , $-TTX$: in the absence of TTX, $+TTX$: in the presence of TTX [Color figure can be viewed at wileyonlinelibrary.com]

DG granule cells, GABA might be expected to only contribute to inhibition of the primary neurons.

Tonic conductance is not only evoked by sIPSC and mIPSC, but also by low concentrations of interstitial GABA activating extrasynaptically-located high-affinity GABA_A receptors or spontaneously opening GABA_A receptors resulting in long-lasting tonic inhibition (Bai et al., 2001; Birnir et al., 1994; Jin, Jin, Kumar-Mendu, et al., 2011; Kasugai et al., 2010; Otis et al., 1991; Semyanov et al., 2003; Soltesz et al., 1995; Włodarczyk et al., 2013). The current density for the extrasynaptic tonic current did not vary along the longitudinal hippocampal axis for neither the DG granule cells nor the CA3 pyramidal neurons. In the DG granule cells the extrasynaptic tonic current was more prominent than in the CA3 pyramidal neurons and may be related to, at least in part, spill-over of GABA from synapses (Brickley et al., 1996; Rossi & Hamann, 1998) as the difference between the two cell-types

disappeared in the presence of TTX. Moreover, extrasynaptic tonic current density positively correlated with total synaptic current density in the ventral DG granule cells. What remained of the current in TTX must have been generated either by spontaneously opening GABA_A receptors channels (Bimir et al., 2000; Korol et al., 2018; Włodarczyk et al., 2013) or interstitial GABA-activated high-affinity GABA_A receptors (Bai et al., 2001; Birnir et al., 1994; Jin, Jin, Kumar-Mendu, et al., 2011; Kasugai et al., 2010; Semyanov et al., 2003). The distinct types of tonic conductances, the sIPSCs, mIPSCs, and extrasynaptic tonic currents, reflect the multimodal nature of the neuronal inhibition present in the hippocampal neurons.

It is possible that some of the functional diversity we identified may be explained by differential expression of GABA_A receptors subtypes in the postsynaptic neurons. Expression of GABA_A receptors varies with developmental stage, brain region, and neuronal types

(Bhandage et al., 2014; Hortnagl et al., 2013; Jin, Bazov, et al., 2011; Wisden, Laurie, Monyer, & Seeburg, 1992). mRNA and protein expression in the dorsal and ventral mouse hippocampus of the various GABA_A subunits has been studied by Hörtnagl et al. (Hortnagl et al., 2013). The $\alpha 2$, $\alpha 5$, and $\gamma 2$ were prominently expressed in the DG granule and CA3 pyramidal layers in both the dorsal and ventral hippocampus (Hortnagl et al., 2013). The $\alpha 1$ and $\alpha 4$ subunits general expression was somewhat lower and considerably weaker in CA3 area as compared to the DG area (Hortnagl et al., 2013). The expression of the $\alpha 3$, $\alpha 6$, and $\gamma 1$ was not detected in the DG or the CA3 area. The δ subunit expression was almost exclusively in the DG granule layer and no labelling was observed in the CA3 area (Hortnagl et al., 2013). The beta subunits were present in both areas and form an integral part of GABA_A receptors (Kasugai et al., 2010). All GABA_A receptors subunits can be found outside of synapses (Kasugai et al., 2010) but some appear to form GABA_A receptors located preferentially outside of synapses. The $\alpha 4$, $\alpha 5$, and the δ subunit are almost exclusively located outside of synapses and, therefore, mainly contribute to extrasynaptic GABA_A receptors generating the extrasynaptic tonic currents, whereas the $\alpha 1$, $\alpha 2$, and $\gamma 2$ subunits form most of the synaptic receptors and thus, generate IPSCs when activated by GABA. The similar expression pattern of the subunits may suggest that the larger dorsal sIPSCs and mIPSCs amplitudes in CA3 pyramidal neurons, as compared to the ventral CA3 hippocampal sIPSCs, can be related to a greater number of receptors at the dorsal postsynaptic sites rather than to an expression of a different subtype of GABA_A receptors in the two regions. In the absence of action potentials, the extrasynaptic tonic current was similar in both cell-types at both the dorsal and the ventral hippocampal pole, despite the GABA_A receptors probably being different, a mix of at least $\alpha 4\beta\delta$, $\alpha 4\beta\gamma 2$, and $\alpha 5\beta\gamma 2$ in the DG granule cells but mainly $\alpha 5\beta\gamma 2$ GABA_A receptors in the CA3 pyramidal neurons. Contributions of $\alpha 4$ and $\alpha 5$ GABA_A receptors to extrasynaptic tonic currents in the hippocampal primary neurons have been reported (Caraiscos et al., 2004; Glykys, Mann, & Mody, 2008; Jin, Jin, Kumar-Mendru, et al., 2011; Mtchedlishvili & Kapur, 2006; Scimemi, Semyanov, Sperk, Kullmann, & Walker, 2005). A recent study has further demonstrated that δ subunit-containing receptors contribute to sIPSCs in DG granule cells to a greater extent than has been previously reported (Sun et al., 2018). Compared to the CA3 pyramidal neurons, the DG granule cells have more subtypes of GABA_A receptors extrasynaptically that may, importantly, vary in affinity for GABA (Jin, Jin, Kumar-Mendru, et al., 2011; Lindquist & Birnir, 2006) enabling greater effective ambient GABA-concentration range in the DG region as compared to the CA3 region.

The dorsal hippocampus is well known for its role in learning and spatial memory formation (Strange et al., 2014) while normal affective processing relies on well-functioning ventral hippocampus where disruption or malfunctioning of ventral hippocampal networks may promote anxiety phenotypes (Papatheodoropoulos, 2018; Zeidler et al., 2018). It is possible that the low tonic GABAergic inhibition we identified in the ventral CA3 neurons may, at least partly, underlie, for example, the higher susceptibility of the ventral hippocampus to generate epileptiform activity.

The findings in this study revealed differential dorsoventral and cell-type specific GABAergic inhibition in two types of the principal neurons in the mouse hippocampal lamellar circuit network. The results are consistent with cell-type specific variation in the inhibitory tone along the longitudinal axis of the mouse hippocampus and are expected to have a significant impact on the different processing of information in the two regions.

ACKNOWLEDGMENTS

The study was funded by Swedish Research Council grants 2018-02952 and 2015-02417 to Bryndis Birnir, the Swedish Brain Foundation grant, Excellence of Diabetes Research in Sweden (EXODIAB) to Bryndis Birnir. We thank professor Costas Papatheodoropoulos for critical comments on the manuscript and Ms. Chang Li for participation in some initial experiments.

CONFLICT OF INTEREST

The authors declare no competing financial interests.

AUTHOR CONTRIBUTIONS

Zhe Jin, Sergiy V. Korol, and Bryndis Birnir designed research; Olga Netsyk, Hayma Hammoud, and Atieh S. Tafreshiha performed research; Olga Netsyk, Hayma Hammoud, Sergiy V. Korol, Zhe Jin, and Bryndis Birnir analyzed data; Olga Netsyk, Hayma Hammoud, and Bryndis Birnir wrote the manuscript with input from all other authors.

DATA AVAILABILITY STATEMENT

The data that support the findings of this study are available from the corresponding author upon reasonable request.

ORCID

Olga Netsyk  <https://orcid.org/0000-0001-6869-7834>

Sergiy V. Korol  <https://orcid.org/0000-0001-8279-2790>

Bryndis Birnir  <https://orcid.org/0000-0002-1763-0266>

REFERENCES

- Andersen, P., Bliss, T. V., & Skrede, K. K. (1971). Lamellar organization of hippocampal pathways. *Experimental Brain Research*, 13(2), 222–238. <https://doi.org/10.1007/bf00234087>
- Andrasfalvy, B. K., & Mody, I. (2006). Differences between the scaling of miniature IPSCs and EPSCs recorded in the dendrites of CA1 mouse pyramidal neurons. *The Journal of Physiology*, 576(Pt 1), 191–196. <https://doi.org/10.1113/jphysiol.2006.115428>
- Bai, D., Zhu, G., Pennefather, P., Jackson, M. F., MacDonald, J. F., & Orser, B. A. (2001). Distinct functional and pharmacological properties of tonic and quantal inhibitory postsynaptic currents mediated by gamma-aminobutyric acid(A) receptors in hippocampal neurons. *Molecular Pharmacology*, 59(4), 814–824. <https://doi.org/10.1124/mol.59.4.814>
- Bhandage, A. K., Jin, Z., Bazov, I., Kononenko, O., Bakalkin, G., Korpi, E. R., & Birnir, B. (2014). GABA-A and NMDA receptor subunit mRNA expression is altered in the caudate but not the putamen of the postmortem brains of alcoholics. *Frontiers in Cellular Neuroscience*, 8, 415. <https://doi.org/10.3389/fncel.2014.00415>
- Birnir, B., Everitt, A. B., & Gage, P. W. (1994). Characteristics of GABA channels in rat dentate gyrus. *The Journal of Membrane Biology*, 142(1), 93–102.

- Birnir, B., Everitt, A. B., Lim, M. S., & Gage, P. W. (2000). Spontaneously opening GABA(a) channels in CA1 pyramidal neurones of rat hippocampus. *The Journal of Membrane Biology*, 174(1), 21–29. <https://doi.org/10.1007/s002320001028>
- Bragdon, A. C., Taylor, D. M., & Wilson, W. A. (1986). Potassium-induced epileptiform activity in area CA3 varies markedly along the septotemporal axis of the rat hippocampus. *Brain Research*, 378(1), 169–173. [https://doi.org/10.1016/0006-8993\(86\)90300-8](https://doi.org/10.1016/0006-8993(86)90300-8)
- Brickley, S. G., Cull-Candy, S. G., & Farrant, M. (1996). Development of a tonic form of synaptic inhibition in rat cerebellar granule cells resulting from persistent activation of GABAA receptors. *The Journal of Physiology*, 497(Pt 3), 753–759. <https://doi.org/10.1113/jphysiol.1996.sp021806>
- Canteras, N. S., & Swanson, L. W. (1992). Projections of the ventral subiculum to the amygdala, septum, and hypothalamus: A PHAL anterograde tract-tracing study in the rat. *The Journal of Comparative Neurology*, 324(2), 180–194. <https://doi.org/10.1002/cne.903240204>
- Caraiscos, V. B., Elliott, E. M., You-Ten, K. E., Cheng, V. Y., Bellelli, D., Newell, J. G., ... Orser, B. A. (2004). Tonic inhibition in mouse hippocampal CA1 pyramidal neurons is mediated by alpha5 subunit-containing gamma-aminobutyric acid type A receptors. *Proceedings of the National Academy of Sciences of the United States of America*, 101(10), 3662–3667. <https://doi.org/10.1073/pnas.0307231101>
- Cossart, R., Hirsch, J. C., Cannon, R. C., Dinocourt, C., Wheal, H. V., Ben-Ari, Y., ... Bernard, C. (2000). Distribution of spontaneous currents along the somato-dendritic axis of rat hippocampal CA1 pyramidal neurons. *Neuroscience*, 99(4), 593–603. [https://doi.org/10.1016/s0306-4522\(00\)00231-1](https://doi.org/10.1016/s0306-4522(00)00231-1)
- Dougherty, K. A., Islam, T., & Johnston, D. (2012). Intrinsic excitability of CA1 pyramidal neurones from the rat dorsal and ventral hippocampus. *The Journal of Physiology*, 590(22), 5707–5722. <https://doi.org/10.1113/jphysiol.2012.242693>
- Edwards, F. A., Konnerth, A., & Sakmann, B. (1990). Quantal analysis of inhibitory synaptic transmission in the dentate gyrus of rat hippocampal slices: A patch-clamp study. *The Journal of Physiology*, 430, 213–249. <https://doi.org/10.1113/jphysiol.1990.sp018289>
- Fanselow, M. S., & Dong, H. W. (2010). Are the dorsal and ventral hippocampus functionally distinct structures? *Neuron*, 65(1), 7–19. <https://doi.org/10.1016/j.neuron.2009.11.031>
- Freund, T. F., & Buzsaki, G. (1996). Interneurons of the hippocampus. *Hippocampus*, 6(4), 347–470. [https://doi.org/10.1002/\(SICI\)1098-1063\(1996\)6:4<347::AID-HIPO1>3.0.CO;2-I](https://doi.org/10.1002/(SICI)1098-1063(1996)6:4<347::AID-HIPO1>3.0.CO;2-I)
- Gilbert, M., Racine, R. J., & Smith, G. K. (1985). Epileptiform burst responses in ventral vs dorsal hippocampal slices. *Brain Research*, 361(1–2), 389–391. [https://doi.org/10.1016/0006-8993\(85\)91309-5](https://doi.org/10.1016/0006-8993(85)91309-5)
- Glykys, J., Mann, E. O., & Mody, I. (2008). Which GABA(a) receptor subunits are necessary for tonic inhibition in the hippocampus? *The Journal of Neuroscience*, 28(6), 1421–1426. <https://doi.org/10.1523/JNEUROSCI.4751-07.2008>
- Hortnagl, H., Berger, M. L., Sperk, G., & Pifl, C. (1991). Regional heterogeneity in the distribution of neurotransmitter markers in the rat hippocampus. *Neuroscience*, 45(2), 261–272. [https://doi.org/10.1016/0306-4522\(91\)90224-c](https://doi.org/10.1016/0306-4522(91)90224-c)
- Hortnagl, H., Tasan, R. O., Wieselthaler, A., Kirchmair, E., Sieghart, W., & Sperk, G. (2013). Patterns of mRNA and protein expression for 12 GABAA receptor subunits in the mouse brain. *Neuroscience*, 236, 345–372. <https://doi.org/10.1016/j.neuroscience.2013.01.008>
- Jin, Z., Bazov, I., Kononenko, O., Korpi, E. R., Bakalkin, G., & Birnir, B. (2011). Selective changes of GABA(A) channel subunit mRNAs in the Hippocampus and orbitofrontal cortex but not in prefrontal cortex of human alcoholics. *Frontiers in Cellular Neuroscience*, 5, 30. <https://doi.org/10.3389/fncel.2011.00030>
- Jin, Z., Jin, Y., & Birnir, B. (2011). GABA-activated single-channel and tonic currents in rat brain slices. *Journal of Visualized Experiments*, (53), e2858. <https://doi.org/10.3791/2858>
- Jin, Z., Jin, Y., Kumar-Mendu, S., Degerman, E., Groop, L., & Birnir, B. (2011). Insulin reduces neuronal excitability by turning on GABA(a) channels that generate tonic current. *PLoS One*, 6(1), e16188. <https://doi.org/10.1371/journal.pone.0016188>
- Kasugai, Y., Swinny, J. D., Roberts, J. D., Dalezios, Y., Fukazawa, Y., Sieghart, W., ... Somogyi, P. (2010). Quantitative localisation of synaptic and extrasynaptic GABAA receptor subunits on hippocampal pyramidal cells by freeze-fracture replica immunolabelling. *The European Journal of Neuroscience*, 32(11), 1868–1888. <https://doi.org/10.1111/j.1460-9568.2010.07473.x>
- Korol, S. V., Jin, Z., Jin, Y., Bhandage, A. K., Tengholm, A., Gandasi, N. R., ... Birnir, B. (2018). Functional characterization of native, high-affinity GABAA receptors in human pancreatic β cells. *eBioMedicine*, 30, 273–282. <https://doi.org/10.1016/j.ebiom.2018.03.014>
- Lathe, R. (2001). Hormones and the hippocampus. *The Journal of Endocrinology*, 169(2), 205–231.
- Lindquist, C. E., & Birnir, B. (2006). Graded response to GABA by native extrasynaptic GABA receptors. *Journal of Neurochemistry*, 97(5), 1349–1356. <https://doi.org/10.1111/j.1471-4159.2006.03811.x>
- Maggio, N., & Segal, M. (2007). Unique regulation of long term potentiation in the rat ventral hippocampus. *Hippocampus*, 17(1), 10–25. <https://doi.org/10.1002/hipo.20237>
- Malik, R., Dougherty, K. A., Parikh, K., Byrne, C., & Johnston, D. (2016). Mapping the electrophysiological and morphological properties of CA1 pyramidal neurons along the longitudinal hippocampal axis. *Hippocampus*, 26(3), 341–361. <https://doi.org/10.1002/hipo.22526>
- Miles, R., Toth, K., Gulyas, A. I., Hajos, N., & Freund, T. F. (1996). Differences between somatic and dendritic inhibition in the hippocampus. *Neuron*, 16(4), 815–823. [https://doi.org/10.1016/s0896-6273\(00\)80101-4](https://doi.org/10.1016/s0896-6273(00)80101-4)
- Milior, G., di Castro, M. A., Sciarria, L. P., Garofalo, S., Branchi, I., Ragozzino, D., ... Maggi, L. (2016). Electrophysiological properties of CA1 pyramidal neurons along the longitudinal Axis of the mouse Hippocampus. *Scientific Reports*, 6, 38242. <https://doi.org/10.1038/srep38242>
- Moser, E., Moser, M. B., & Andersen, P. (1993). Spatial learning impairment parallels the magnitude of dorsal hippocampal lesions, but is hardly present following ventral lesions. *The Journal of Neuroscience*, 13(9), 3916–3925.
- Mtchedlishvili, Z., & Kapur, J. (2006). High-affinity, slowly desensitizing GABAA receptors mediate tonic inhibition in hippocampal dentate granule cells. *Molecular Pharmacology*, 69(2), 564–575. <https://doi.org/10.1124/mol.105.016683>
- Neddens, J., & Buonanno, A. (2010). Selective populations of hippocampal interneurons express ErbB4 and their number and distribution is altered in ErbB4 knockout mice. *Hippocampus*, 20(6), 724–744. <https://doi.org/10.1002/hipo.20675>
- Otis, T. S., & Mody, I. (1992). Modulation of decay kinetics and frequency of GABAA receptor-mediated spontaneous inhibitory postsynaptic currents in hippocampal neurons. *Neuroscience*, 49(1), 13–32. [https://doi.org/10.1016/0306-4522\(92\)90073-b](https://doi.org/10.1016/0306-4522(92)90073-b)
- Otis, T. S., Staley, K. J., & Mody, I. (1991). Perpetual inhibitory activity in mammalian brain slices generated by spontaneous GABA release. *Brain Research*, 545(1–2), 142–150. [https://doi.org/10.1016/0006-8993\(91\)91280-e](https://doi.org/10.1016/0006-8993(91)91280-e)
- Overstreet-Wadiche, L. S., & Westbrook, G. L. (2006). Functional maturation of adult-generated granule cells. *Hippocampus*, 16(3), 208–215. <https://doi.org/10.1002/hipo.20152>
- Papatheodoropoulos, C. (2015). Striking differences in synaptic facilitation along the dorsoventral axis of the hippocampus. *Neuroscience*, 301, 454–470. <https://doi.org/10.1016/j.neuroscience.2015.06.029>
- Papatheodoropoulos, C. (2018). Electrophysiological evidence for long-axis intrinsic diversification of the hippocampus. *Frontiers in Bioscience (Landmark Ed)*, 23, 109–145. <https://doi.org/10.2741/4584>
- Papatheodoropoulos, C., Asproдини, E., Nikita, I., Koutsona, C., & Kostopoulos, G. (2002). Weaker synaptic inhibition in CA1 region of

- ventral compared to dorsal rat hippocampal slices. *Brain Research*, 948 (1–2), 117–121. [https://doi.org/10.1016/s0006-8993\(02\)02958-x](https://doi.org/10.1016/s0006-8993(02)02958-x)
- Pavlov, I., Savtchenko, L. P., Kullmann, D. M., Semyanov, A., & Walker, M. C. (2009). Outwardly rectifying tonically active GABAA receptors in pyramidal cells modulate neuronal offset, not gain. *The Journal of Neuroscience*, 29(48), 15341–15350. <https://doi.org/10.1523/JNEUROSCI.2747-09.2009>
- Paxinos, G., & Watson, C. (1986). *The Rat Brain in Stereotaxic Coordinates*, 2nd ed., Cambridge, MA: Academic Press.
- Pedroni, A., Minh do, D., Mallamaci, A., & Cherubini, E. (2014). Electrophysiological characterization of granule cells in the dentate gyrus immediately after birth. *Frontiers in Cellular Neuroscience*, 8, 44. <https://doi.org/10.3389/fncel.2014.00044>
- Petrides, T., Georgopoulos, P., Kostopoulos, G., & Papatheodoropoulos, C. (2007). The GABAA receptor-mediated recurrent inhibition in ventral compared with dorsal CA1 hippocampal region is weaker, decays faster and lasts less. *Experimental Brain Research*, 177(3), 370–383. <https://doi.org/10.1007/s00221-006-0681-6>
- Preston, A. R., & Eichenbaum, H. (2013). Interplay of hippocampus and prefrontal cortex in memory. *Current Biology*, 23(17), R764–R773. <https://doi.org/10.1016/j.cub.2013.05.041>
- Risold, P. Y., & Swanson, L. W. (1996). Structural evidence for functional domains in the rat hippocampus. *Science*, 272(5267), 1484–1486.
- Rossi, D. J., & Hamann, M. (1998). Spillover-mediated transmission at inhibitory synapses promoted by high affinity alpha6 subunit GABA(a) receptors and glomerular geometry. *Neuron*, 20(4), 783–795. [https://doi.org/10.1016/s0896-6273\(00\)81016-8](https://doi.org/10.1016/s0896-6273(00)81016-8)
- Schreurs, A., Sabanov, V., & Balschun, D. (2017). Distinct properties of long-term potentiation in the dentate Gyrus along the Dorsoventral Axis: Influence of age and inhibition. *Scientific Reports*, 7(1), 5157. <https://doi.org/10.1038/s41598-017-05358-1>
- Scimemi, A., Semyanov, A., Sperk, G., Kullmann, D. M., & Walker, M. C. (2005). Multiple and plastic receptors mediate tonic GABAA receptor currents in the hippocampus. *The Journal of Neuroscience*, 25(43), 10016–10024. <https://doi.org/10.1523/JNEUROSCI.2520-05.2005>
- Semyanov, A., Walker, M. C., & Kullmann, D. M. (2003). GABA uptake regulates cortical excitability via cell type-specific tonic inhibition. *Nature Neuroscience*, 6(5), 484–490. <https://doi.org/10.1038/nn1043nn1043>
- Soltész, I., Smetters, D. K., & Mody, I. (1995). Tonic inhibition originates from synapses close to the soma. *Neuron*, 14(6), 1273–1283. [https://doi.org/10.1016/0896-6273\(95\)90274-0](https://doi.org/10.1016/0896-6273(95)90274-0)
- Sotiriou, E., Papatheodoropoulos, C., & Angelatou, F. (2005). Differential expression of gamma-aminobutyric acid--a receptor subunits in rat dorsal and ventral hippocampus. *Journal of Neuroscience Research*, 82 (5), 690–700. <https://doi.org/10.1002/jnr.20670>
- Staley, K. J., & Mody, I. (1992). Shunting of excitatory input to dentate gyrus granule cells by a depolarizing GABAA receptor-mediated post-synaptic conductance. *Journal of Neurophysiology*, 68(1), 197–212. <https://doi.org/10.1152/jn.1992.68.1.197>
- Staley, K. J., Soldo, B. L., & Proctor, W. R. (1995). Ionic mechanisms of neuronal excitation by inhibitory GABAA receptors. *Science*, 269(5226), 977–981. <https://doi.org/10.1126/science.7638623>
- Stell, B. M., Brickley, S. G., Tang, C. Y., Farrant, M., & Mody, I. (2003). Neuroactive steroids reduce neuronal excitability by selectively enhancing tonic inhibition mediated by delta subunit-containing GABAA receptors. *Proceedings of the National Academy of Sciences of the United States of America*, 100(24), 14439–14444. <https://doi.org/10.1073/pnas.2435457100>
- Strange, B. A., Witter, M. P., Lein, E. S., & Moser, E. I. (2014). Functional organization of the hippocampal longitudinal axis. *Nature Reviews Neuroscience*, 15(10), 655–669. <https://doi.org/10.1038/nrn3785>
- Sun, M. Y., Shu, H. J., Benz, A., Bracamontes, J., Akk, G., Zorumski, C. F., ... Mennerick, S. J. (2018). Chemogenetic isolation reveals synaptic contribution of delta GABAA receptors in mouse dentate granule neurons. *The Journal of Neuroscience*, 38(38), 8128–8145. <https://doi.org/10.1523/JNEUROSCI.0799-18.2018>
- Ting, J. T., Daigle, T. L., Chen, Q., & Feng, G. (2014). Acute brain slice methods for adult and aging animals: application of targeted patch clamp analysis and optogenetics. *Methods Mol Biol*, 1183, 221–242.
- Williams, S. R., Buhl, E. H., & Mody, I. (1998). The dynamics of synchronized neurotransmitter release determined from compound spontaneous IPSCs in rat dentate granule neurones in vitro. *The Journal of Physiology*, 510 (Pt 2), 477–497. <https://doi.org/10.1111/j.1469-7793.1998.477bk.x>
- Wisden, W., Laurie, D. J., Monyer, H., & Seeburg, P. H. (1992). The distribution of 13 GABAA receptor subunit mRNAs in the rat brain. I. Telencephalon, diencephalon, mesencephalon. *The Journal of Neuroscience*, 12(3), 1040–1062.
- Włodarczyk, A. I., Sylantyev, S., Herd, M. B., Kersante, F., Lambert, J. J., Rusakov, D. A., ... Walker, M. C. (2013). GABA-independent GABAA receptor openings maintain tonic currents. *The Journal of Neuroscience*, 33(9), 3905–3914. <https://doi.org/10.1523/JNEUROSCI.4193-12.2013>
- Zeidler, Z., Brandt-Fontaine, M., Leintz, C., Krook-Magnuson, C., Netoff, T., & Krook-Magnuson, E. (2018). Targeting the mouse ventral hippocampus in the intrahippocampal kainic acid model of temporal lobe epilepsy. *eNeuro*, 5(4), 1–16. <https://doi.org/10.1523/ENEURO.0158-18.2018>

SUPPORTING INFORMATION

Additional supporting information may be found online in the Supporting Information section at the end of this article.

How to cite this article: Netsyk O, Hammoud H, Korol SV, Jin Z, Tafreshiha AS, Birnir B. Tonic GABA-activated synaptic and extrasynaptic currents in dentate gyrus granule cells and CA3 pyramidal neurons along the mouse hippocampal dorsoventral axis. *Hippocampus*. 2020;30:1146–1157. <https://doi.org/10.1002/hipo.23245>